1

Frequency Domain Turbo Equalization with Iterative Channel Estimation for MIMO Underwater Acoustic Communications

Zhenrui Chen, Student Member, IEEE, Jintao Wang, Senior Member, IEEE, and Yahong Rosa Zheng, Fellow, IEEE

Abstract

This paper proposes a new iterative receiver for single carrier multiple-input multiple-output (SC-MIMO) underwater acoustic (UWA) communications, which utilizes frequency domain turbo equalization (FDTE) and iterative channel estimation. Soft decision symbols are not only fed back to the equalizer to cancel the inter-symbol interference (ISI) and co-channel interference (CCI), but also used as training signals in the channel estimator to update the estimated channel state information (CSI) after each turbo iteration. This iterative channel estimation scheme helps to combat the problem commonly suffered by block-processing receivers in fast time-varying channels. Compared with time domain turbo equalization, frequency domain turbo equalization achieves comparable performance with significantly reduced computational complexity. Using soft decision symbols to re-estimate the time varying channels, iterative channel estimation further improves the accuracy of the estimated CSI. The proposed iterative receiver has been verified through undersea experimental data collected in the Surface Processes and Acoustic Communications Experiment 2008 (SPACE08).

Index Terms

Underwater acoustic (UWA) communications, multiple-input multiple-output (MIMO), turbo equalization, frequency domain equalization, iterative channel estimation

Z. Chen and J. Wang are with the Department of Electronic Engineering, Tsinghua University, Beijing 100084, China (e-mail: chenzr08@gmail.com; wangjintao@tsinghua.edu.cn).

Y.R. Zheng is with the Department of Electrical and Computer Engineering, Missouri University of Science and Technology, Rolla, MO 65409, USA (e-mail: zhengyr@mst.edu).

I. Introduction

Underwater acoustic (UWA) channels present many challenges for reliable high data-rate communications [1]–[5]. The UWA channels are characterized by extended multipath leading to long delay spread, and rapid time variation due to significant Doppler effects. Single carrier (SC) transmission with frequency domain equalization (FDE) has drawn great attention as an attractive alternative to OFDM, especially in the uplink of radio frequency communications, and underwater acoustic communications [6]–[8]. Turbo equalization is originally proposed in the time domain equalization (TDE) and then extended to frequency domain equalization (FDE) to achieve satisfactory performance for SC systems [9]–[12]. A low-complexity equalizer based on linear filtering is utilized to replace the maximum *a posteriori* probability equalizer under the minimum mean squared error (MMSE) criterion for single-input single-output (SISO) systems [9]. By subtracting *a priori* mean of the co-channel interference (CCI) using parallel interference cancellation (PIC), the linear MMSE turbo equalization is extended to multiple-input multiple-output (MIMO) systems, also termed as TDE-PIC [10]. Soft-feedback equalizer combines soft decisions with *a priori* information for inter-symbol interference (ISI) cancellation, using a statistical model for the equalizer outputs and *a priori* information [11]. A low-complexity MMSE-based soft-decision feedback turbo equalizer is extended from BPSK to multilevel modulations [12].

For communication systems with long delay spread, the computational complexity of turbo equalization performed in the time domain is prohibitively high [13]. Frequency domain turbo equalization (FDTE) reduces the complexity while comparable performance is achieved [14]-[19]. An iterative block decision feedback equalization (DFE) performs both the feedforward and feedback filtering in the frequency domain, leading to a significant reduction of complexity [14]. Two frequency domain DFE schemes with pilot-assisted channel estimation are proposed based on time domain decision feedback and frequency domain decision feedback (FDE-FDDF), respectively [15]. A simplified parameter estimation method is introduced to calculate the coefficients of the feedforward and feedback filters, further reducing the implementation complexity of the FDE-FDDF scheme [16]. By considering the reliability of the decision feedback symbols, a general framework for iterative block-wise equalization is proposed for MIMO systems [17]. Four block-wise DFE schemes are optimized under the MMSE criterion and proved to be equivalent. Combining with phase rotation compensation and soft successive interference cancellation, a layered FDTE structure is proposed to cope with unbalanced MIMO channels [18]. Three block-wise FDTE schemes with soft interference cancellation are introduced, and a suboptimal bin-wise FDTE scheme is proposed to achieve complexity-performance tradeoff [19]. Several turbo equalization schemes have been adopted to UWA communications [10], [18], [20]-[22]. Turbo equalization schemes for SC UWA systems are reviewed with linear equalizers and soft decision feedback equalizers in both the time and frequency domains [23].

In the previous work of turbo equalization [9]–[12], perfect channel state information (CSI) is assumed to be available at the receiver. For practical systems, however, the CSI is obtained using various channel estimation methods. The scaled least squares (LS) and relaxed MMSE methods are proposed for MIMO systems, offering tradeoff between performance and the required prior knowledge of channel parameters [24]. Using a path-based channel model, compressed sensing techniques with overcomplete dictionaries are adopted to deal with channels with larger Doppler spread [25]. Extending the path-based channel model, a channel variation model is proposed that channel paths within a cluster share the same amplitude, delay, and Doppler scale variations, and each cluster varies independently [26]. By parameterizing the amplitude variation and delay variation of each path with polynomial approximation, the two-stage sparse channel estimation approach reduces the number of candidates on the delay-Doppler search grid [27]. By combining natural gradient adaptation and L_0 -norm regularization, an algorithmic framework for sparse adaptive algorithms is introduced [28].

For block transmission systems in UWA communications [4]–[7], channel estimation is conducted based on pilots or training signals, and the CSI is treated as time invariant in one block. However, due to the time-varying characteristic of UWA channels, the channel changes in the block, and the instantaneous CSI during the payload transmission is slightly different from the estimated CSI. By using the time invariant assumption, block-wise systems with conventional channel estimation methods suffer performance degradation, especially for UWA systems using turbo equalization [10], [18]. During the iterations of turbo equalization, the estimated CSI has not been updated, termed as non-iterative channel estimation (NCE). Compared with NCE methods, iterative channel estimation (ICE) during turbo equalization improves the accuracy of the estimated CSI, using soft decision symbols as training signals to re-estimate the channels at each iteration [29]. The normalized least mean squares (NLMS) and improved proportionate NLMS algorithms are adopted for iterative channel estimation in time domain turbo equalization [30].

In this paper, we propose an iterative receiver for single carrier MIMO (SC-MIMO) systems, combining frequency domain turbo equalization with iterative channel estimation. Although the primary idea was published in [1], the paper presents more details of the undersea experiment, detailed derivations and explanations of the algorithm, and more solid results of experimental data processing, especially on the comparison of different turbo equalization schemes and iterative channel estimation algorithms to improve the performance. Unlike the previous FDE-FDDF schemes [15]–[17], multilevel modulations such as 8PSK and 16QAM are considered in this paper. Soft decision symbols are not only fed back

to the equalizer to cancel the ISI and CCI, but also used as training signals in the channel estimator to update the estimated CSI. Compared with time domain turbo equalization, frequency domain turbo equalization reduces the complexity significantly, while comparable performance is achieved. Using pilots at the first iteration and soft decision symbols in the following iterations, iterative channel estimation further improves the accuracy of the estimated CSI. The proposed iterative receiver has been verified through undersea experimental data collected in the Surface Processes and Acoustic Communications Experiment 2008 (SPACE08).

The rest of this paper is organized as follows. Section II introduces the overview of block transmission SC-MIMO systems including the transmitter and the iterative receiver. Frequency domain turbo equalization and iterative channel estimation are presented in Section III and Section IV, respectively. Computational complexity of turbo equalization schemes and iterative channel estimation algorithms is analyzed in Sections V. Data processing results of the SPACE08 experiment performed with the iterative receiver are demonstrated in Sections VI. Finally, Section VII concludes the paper.

Notation: Bold letters stand for matrices and vectors. The operators $(\cdot)^*$, $(\cdot)^T$, and $(\cdot)^H$ denote conjugate, transpose, and Hermitian transpose, respectively. The identity matrix with size $K \times K$ is denoted as \mathbf{I}_K , and the zero matrix with size $M \times N$ is denoted as $\mathbf{0}_{M \times N}$. The (m, n)-th element of the matrix \mathbf{A} is denoted as $\mathbf{A}[m, n]$. The $M \times M$ diagonal matrix with diagonal elements b_1, b_2, \cdots, b_M is denoted by $\mathbf{B} = \mathrm{diag}\{b_1, b_2, \cdots, b_M\}$. The block diagonal matrix where submatrices $\mathbf{A}_1, \mathbf{A}_2, \cdots, \mathbf{A}_K$ are on the main diagonal is denoted by $\mathbf{A} = \mathrm{Bdiag}\{\mathbf{A}_k\}_{k=1}^K$. The operation $\mathbf{A} \otimes \mathbf{B}$ denotes the Kronecker product of \mathbf{A} and \mathbf{B} . The cross-covariance matrix between two vectors \mathbf{x} and \mathbf{y} is defined as $\mathrm{Cov}(\mathbf{x}, \mathbf{y}) = \mathrm{E}\{(\mathbf{x} - \mathrm{E}\{\mathbf{x}\})(\mathbf{y} - \mathrm{E}\{\mathbf{y}\})^H\}$, where $\mathrm{E}\{\mathbf{x}\}$ is the statistical expectation of \mathbf{x} .

II. BLOCK TRANSMISSION SC-MIMO SYSTEMS

Consider the SC-MIMO system with M transducers at the transmitter and N hydrophones at the receiver. Fig. 1 depicts structures of the transmitter and the receiver in the SC-MIMO system. At the transmitter, each bit stream is independently encoded, interleaved, and mapped, as shown in Fig 1(a). In this paper, convolutional code and random interleaver are used in the MIMO system. However, the design of turbo equalization is independent of channel coding schemes. The convolutional code can be replaced with other channel coding schemes, such as low-density parity-check (LDPC) code, turbo code, and polar code. For the m-th bit stream ($m=1,2,\cdots,M$), input bits to the mapper are denoted by \mathbf{c}^m . For a 2^Q -ary modulation with the constellation set $\mathcal{S}=\{\alpha_1,\alpha_2,\cdots,\alpha_{2^Q}\}$, every Q bits $\mathbf{c}_k^m=[c_{k,1}^m,c_{k,2}^m,\cdots,c_{k,Q}^m]$ are mapped into the symbol $x_{m,k}$ with k being the time instant. The constellation set is normalized to unit energy as $\mathbf{E}\{|x_{m,k}|^2\}=1$. The modulated symbols are grouped into data blocks with length K.

Gap whose length is larger than the channel length is inserted between data blocks and pilots to avoid inter-block interference. The M streams are transmitted at the same time and with the same frequency, thus both ISI and CCI are introduced in the SC-MIMO communication system.

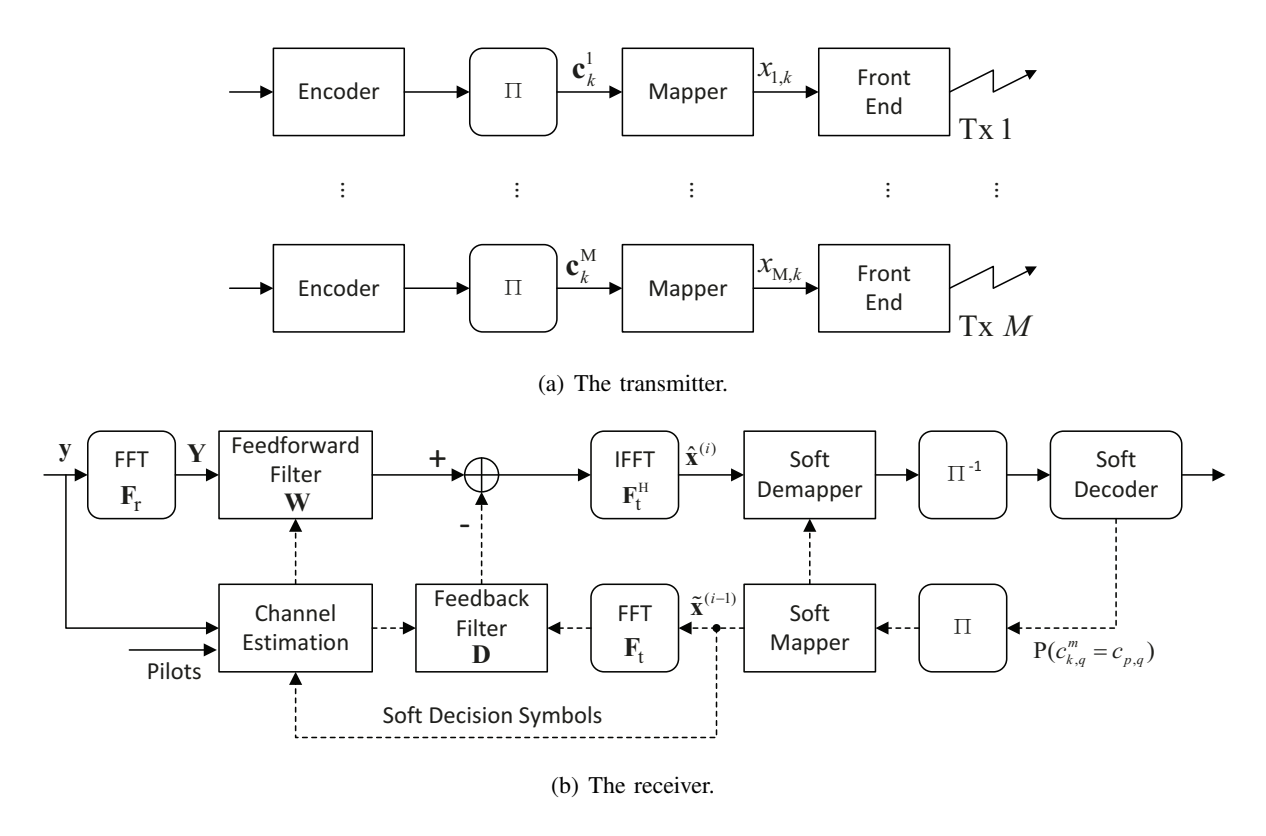


Fig. 1. Block diagram of the SC-MIMO systems.

We propose an iterative receiver structure for SC-MIMO systems to achieve satisfactory performance. Soft decision symbols obtained at the previous iteration are not only fed back to the equalizer to cancel the ISI and CCI, but also used as training signals in the channel estimator to re-estimate the UWA channels. A front-end module is employed to preprocess received passband signals to synchronize, convert into baseband, and compensate for dilation or compression. After that, frequency domain decision feedback equalization, soft demapping, soft decoding, and iterative channel estimation are performed as shown in Fig. 1(b). Using output symbols of the equalizer, the log-likelihood ratio (LLR) of coded bits is calculated in the demapper and utilized for decoding. The soft-input soft output decoder is adopted to generate new extrinsic information, which is fed back to the soft mapper and mapped into soft decision symbols. At the next iteration, soft decision symbols are not only fed back to cancel the ISI and CCI, but also used as training signals to update the estimation of CSI.

III. FREQUENCY DOMAIN TURBO EQUALIZATION

This section describes the SC-MIMO systems using frequency domain turbo equalization. System model of the block transmission, the FDE-FDDF scheme, and demapping and decoding will be presented in the following subsections, respectively.

A. System Model

Assuming symbol-rate sampling, the baseband equivalent signal of the n-th receive hydrophone at time instant k can be expressed as

$$r_{n,k} = \sum_{m=1}^{M} \sum_{l=0}^{L-1} h_{n,m}^{(l)} x_{m,k-l} + w_{n,k},$$
(1)

where L is the length of the channel impulse response (CIR), $\{h_{n,m}^{(l)}\}_{l=0}^{L-1}$ is the CIR of the subchannel between the m-th transmit transducer and the n-th receive hydrophone, and $w_{n,k}$ is the additive white Gaussian noise (AWGN) with zero mean and variance σ^2 . The received signals $\mathbf{r}_k = [r_{1,k}, r_{2,k}, \cdots, r_{N,k}]^{\mathrm{T}}$ can be written into the matrix form as

$$\mathbf{r}_k = \sum_{l=0}^{L-1} \mathbf{h}^{(l)} \mathbf{x}_{k-l} + \mathbf{w}_k, \tag{2}$$

where $\mathbf{x}_k = [x_{1,k}, x_{2,k}, \cdots, x_{M,k}]^T$ is the vector of transmitted symbols at time instant k, and the l-th delay channel matrix $\mathbf{h}^{(l)}$ is given as

$$\mathbf{h}^{(l)} = \begin{bmatrix} h_{1,1}^{(l)} & \cdots & h_{1,M}^{(l)} \\ \vdots & \ddots & \vdots \\ h_{N,1}^{(l)} & \cdots & h_{N,M}^{(l)} \end{bmatrix}.$$
 (3)

Using the overlap-add method as in zero padding OFDM (ZP-OFDM) [31], the received signals are reformed as

$$\mathbf{y} = [\mathbf{r}_1^{\mathrm{T}}, \cdots, \mathbf{r}_K^{\mathrm{T}}]^{\mathrm{T}} + [\mathbf{r}_{K+1}^{\mathrm{T}}, \cdots, \mathbf{r}_{K+K_{\mathrm{g}}}^{\mathrm{T}}, \mathbf{0}_{1 \times (K-K_{\mathrm{g}})}]^{\mathrm{T}}.$$
 (4)

Linear convolution of transmitted symbols and CIR are converted into circular convolution, which makes frequency domain processing available. Thus, the SC-MIMO system can be modeled as

$$y = hx + w, (5)$$

where $\mathbf{x} = [\mathbf{x}_1^{\mathrm{T}}, \mathbf{x}_2^{\mathrm{T}}, \cdots, \mathbf{x}_K^{\mathrm{T}}]^{\mathrm{T}}$ and $\mathbf{y} = [\mathbf{y}_1^{\mathrm{T}}, \mathbf{y}_2^{\mathrm{T}}, \cdots, \mathbf{y}_K^{\mathrm{T}}]^{\mathrm{T}}$ are the concatenated transmitted symbols and received symbols, respectively. The time domain channel matrix \mathbf{h} is a block circulant matrix with $[\mathbf{h}_0^{\mathrm{T}}, \cdots, \mathbf{h}_{L-1}^{\mathrm{T}}, \mathbf{0}_{M \times (N(K-L))}]^{\mathrm{T}}$ as its first column. However, the overlap-add step leads to slight performance degradation by coloring the noise terms, which can be observed in Section VI. In this paper,

we still treat noise in the reformed received signals as independent and identically distributed (i.i.d.) Gaussian distribution $\mathcal{N}(0, \sigma^2)$ to simplify the derivation.

To detect transmitted symbols \mathbf{x} from the reformed received signals \mathbf{y} , frequency domain equalization schemes are often used due to the low computational complexity. Denote the K-point normalized fast Fourier transform (FFT) matrix as \mathbf{F} , whose (k_1,k_2) -th element is $\frac{1}{\sqrt{K}}\exp\left\{-2\pi\frac{\sqrt{-1}(k_1-1)(k_2-1)}{K}\right\}$. The block FFT matrix for transmitted symbols and received signals are defined as $\mathbf{F}_t = \mathbf{F} \otimes \mathbf{I}_M$ and $\mathbf{F}_r = \mathbf{F} \otimes \mathbf{I}_N$, respectively. Transforming the time-domain signals in (5) into frequency domain yields

$$\mathbf{Y} = \mathbf{H}\mathbf{F}_{\mathbf{t}}\mathbf{x} + \mathbf{F}_{\mathbf{r}}\mathbf{w},\tag{6}$$

where $\mathbf{Y} = \mathbf{F}_r \mathbf{y} = [\mathbf{Y}_1^T, \mathbf{Y}_2^T, \cdots, \mathbf{Y}_K^T]^T$ is the block FFT of the received signals, and $\mathbf{H} = \mathbf{F}_r \mathbf{h} \mathbf{F}_t^H$ is the frequency domain channel matrix. Since \mathbf{h} is a block circulant matrix, \mathbf{H} is a block diagonal matrix and $\mathbf{H} = \mathrm{Bdiag}\{\mathbf{H}_k\}_{k=1}^K$ with \mathbf{H}_k being $N \times M$ matrices.

B. Frequency Domain Equalization with Frequency Domain Decision Feedback

Soft decision symbols obtained at the previous iteration are used to cancel the ISI and CCI at the current iteration. The FDTE schemes process the received signals \mathbf{Y} in the frequency domain and utilize feedback symbols $\tilde{\mathbf{x}}^{(i-1)}$ obtained at the (i-1)-th iteration to improve the detection of the transmitted symbols. Using the FDE-FDDF scheme, the output of the equalizer at the i-th iteration can be written as [15]

$$\hat{\mathbf{x}}^{(i)} = \mathbf{F}_{t}^{H}(\mathbf{W}\mathbf{Y} - \mathbf{D}\mathbf{F}_{t}\tilde{\mathbf{x}}^{(i-1)}),\tag{7}$$

where the block diagonal matrices $\mathbf{W} = \mathrm{Bdiag}\{\mathbf{W}_k\}_{k=1}^K$ and $\mathbf{D} = \mathrm{Bdiag}\{\mathbf{D}_k\}_{k=1}^K$ are feedforward and feedback matrices, respectively, which will be jointly optimized according to the MMSE criterion. The time domain feedback matrix $\mathbf{G} = \mathbf{F}_t^H \mathbf{D} \mathbf{F}_t$ is a block circulant matrix, and its diagonal elements are set to zero to avoid self-subtraction of the desired symbol by its previous estimation [15]. Consequently, the frequency domain feedback matrix is a block diagonal matrix with the following constraints

$$\sum_{k=1}^{K} \mathbf{D}_{k}[m, m] = 0, \quad m = 1, 2, \cdots, M.$$
(8)

Two important correlation matrices of transmitted symbols and feedback symbols are defined as $\mathbf{B}^{(i-1)} = \mathrm{E}\{\tilde{\mathbf{x}}^{(i-1)}(\tilde{\mathbf{x}}^{(i-1)})^{\mathrm{H}}\}$, and $\mathbf{\Theta}^{(i-1)} = \mathrm{E}\{\mathbf{x}(\tilde{\mathbf{x}}^{(i-1)})^{\mathrm{H}}\}$. In the rest of this paper, superscripts of correlation matrices are omitted for brevity. Due to the random interleaver, we assume soft decision symbols are uncorrelated with transmitted symbols at different transducers or at different time instants.

Further, the reliability of soft decision symbols for the same transducer is assumed to be the same for different time instants. Thus, the correlation matrices are written as

$$\mathbf{B} = \mathbf{I}_N \otimes \mathbf{B}_0, \quad \mathbf{B}_0 = \operatorname{diag}\{\beta_1, \beta_2, \cdots, \beta_M\},\$$

$$\mathbf{\Theta} = \mathbf{I}_N \otimes \mathbf{\Theta}_0, \quad \mathbf{\Theta}_0 = \operatorname{diag}\{\theta_1, \theta_2, \cdots, \theta_N\},\$$
(9)

where the elements of \mathbf{B}_0 and $\mathbf{\Theta}_0$ are obtained by

$$E\{\tilde{x}_{m,k}^{(i-1)}(\tilde{x}_{m',k'}^{(i-1)})^*\} = \beta_m \delta_{m,m'} \delta_{k,k'},$$

$$E\{x_{m,k}(\tilde{x}_{m',k'}^{(i-1)})^*\} = \theta_m \delta_{m,m'} \delta_{k,k'},$$
(10)

and $\delta_{m,m'}=1$ if and only if m=m'.

The minimization problem subject to equality constraints is solved by using the Lagrange multipliers method. The equivalent optimization problem is to minimize the mean square error (MSE) of equalized symbols at the i-th iteration with Lagrange multipliers as

$$\min_{\mathbf{W}, \mathbf{D}} \left\{ \mathrm{E}\{(\hat{\mathbf{x}}^{(i)} - \mathbf{x})^{\mathrm{H}}(\hat{\mathbf{x}}^{(i)} - \mathbf{x})\} + \sum_{m=1}^{M} \lambda_m \left\{ \sum_{k=1}^{K} \mathbf{D}_k[m, m] \right\} \right\}.$$
(11)

The feedforward and feedback matrices are found to be

$$\mathbf{W}_{k} = (\mathbf{I}_{M} + \mathbf{D}_{k} \mathbf{\Theta}_{0}^{\mathrm{H}}) \mathbf{H}_{k}^{\mathrm{H}} (\mathbf{H}_{k} \mathbf{H}_{k}^{\mathrm{H}} + \sigma^{2} \mathbf{I}_{N})^{-1},$$

$$\mathbf{D}_{k} = \hat{\mathbf{D}}_{k} - \mathbf{\Lambda} \check{\mathbf{D}}_{k},$$
(12)

where $\hat{\mathbf{D}}_k = \mathbf{\Gamma}_k \mathbf{B}_0 \check{\mathbf{D}}_k$, $\check{\mathbf{D}}_k = (\mathbf{B}_0 - \mathbf{\Theta}_0^H \mathbf{\Gamma}_k \mathbf{\Theta}_0)^{-1}$, $\mathbf{\Gamma}_k = \mathbf{H}_k^H (\mathbf{H}_k \mathbf{H}_k^H + \sigma^2 \mathbf{I}_N)^{-1} \mathbf{H}_k$, and the Lagrange multiplier $\mathbf{\Lambda} = \mathrm{diag}\{\lambda_1, \lambda_2, \cdots, \lambda_M\}$ is obtained as

$$\lambda_{m} = \frac{\sum_{k=1}^{K} \hat{\mathbf{D}}_{k}[m, m]}{\sum_{k=1}^{K} \check{\mathbf{D}}_{k}[m, m]}.$$
(13)

When soft decision symbols are unavailable at the initial iteration, the feedforward matrix and feedback matrix are given under the MMSE criterion as

$$\mathbf{W}_{k} = \mathbf{H}_{k}^{H} (\mathbf{H}_{k} \mathbf{H}_{k}^{H} + \sigma^{2} \mathbf{I}_{N})^{-1},$$

$$\mathbf{D}_{k} = \mathbf{0}_{M \times M}.$$
(14)

In this case, the FDE-FDDF scheme reduces to the traditional frequency domain linear equalization, which can be treated as the MMSE estimation of transmitted symbols without the prior information.

Compared with the traditional frequency domain linear equalization, the FDE-FDDF scheme obtains soft decision symbols at the previous iteration, and utilizes the prior information via the feedforward and

feedback matrices to improve the performance of the current iteration, rather than the traditional MMSE estimation in (14). Intuitively, the received signals are filtered in the frequency domain as

$$\mathbf{WY} = (\mathbf{I}_{MK} + \mathbf{D}\mathbf{\Theta}^{\mathrm{H}})\mathbf{H}^{\mathrm{H}}(\mathbf{H}\mathbf{H}^{\mathrm{H}} + \sigma^{2}\mathbf{I}_{NK})^{-1}\mathbf{Y}, \tag{15}$$

where the term $\mathbf{H}^{\mathrm{H}}(\mathbf{H}\mathbf{H}^{\mathrm{H}} + \sigma^{2}\mathbf{I}_{NK})^{-1}\mathbf{Y} \triangleq \check{\mathbf{X}} \triangleq \mathbf{F}_{\mathrm{t}}\check{\mathbf{x}}$ can be treated as the MMSE estimation of transmitted symbols without the prior information, which is also known as frequency domain linear equalization. Therefore, the output of the feedforward filter can be divided into two parts as $\mathbf{W}\mathbf{Y} = \mathbf{F}_{\mathrm{t}}\check{\mathbf{x}} + \mathbf{D}\mathbf{\Theta}^{\mathrm{H}}\mathbf{F}_{\mathrm{t}}\check{\mathbf{x}}$, where $\mathbf{\Theta} = \mathrm{E}\{\mathbf{x}(\check{\mathbf{x}}^{(i-1)})^{\mathrm{H}}\}$ is the cross-correlation matrix of the transmitted symbols \mathbf{x} and feedback symbols $\check{\mathbf{x}}^{(i-1)}$. Consequently, the final output of the equalizer in (7) is rewritten as

$$\hat{\mathbf{x}}^{(i)} = \breve{\mathbf{x}} + \mathbf{F}_{t}^{H} \mathbf{D} \mathbf{E} \{ \tilde{\mathbf{x}}^{(i-1)} \mathbf{x}^{H} \} \mathbf{F}_{t} \breve{\mathbf{x}} - \mathbf{F}_{t}^{H} \mathbf{D} \mathbf{F}_{t} \tilde{\mathbf{x}}^{(i-1)}.$$
(16)

Since the constellation set is normalized to unit energy as $E\{|x_{m,k}|^2\}=1$, the second term in (16) is approximately equal to the third term thus canceling out. As a result, the output of the equalizer is a very close estimation of the transmitted symbols \mathbf{x} , as the prior information of \mathbf{x} in the previous iteration converges to the transmitted symbols.

C. Demapping and Decoding

At the *i*-th iteration, the equalized symbol $\hat{x}_{m,k}^{(i)}$ is assumed to be the output of an equivalent AWGN channel and treated as a random variable with Gaussian distribution $\mathcal{N}(\mu_{m,k}x_{m,k}, \sigma_{m,k}^2)$ [9]. The calculation of $\mu_{m,k}$ and $\sigma_{m,k}^2$ in the FDE-FDDF scheme will be demonstrated later. As a result, the conditional probability of equalized symbols is calculated using the Gaussian distribution assumption as

$$P(\hat{x}_{m,k}^{(i)}|x_{m,k} = \alpha_p) = \frac{1}{\pi \sigma_{m,k}^2} \exp\left\{-\frac{|\hat{x}_{m,k}^{(i)} - \mu_{m,k} \alpha_p|^2}{\sigma_{m,k}^2}\right\}.$$
 (17)

Extrinsic information of the coded bit is demapped from the equalized symbol as [9]

$$L_{e}(c_{k,q}^{m}) = \ln \frac{\sum_{\alpha_{p}: c_{p,q}=0} P(\hat{x}_{m,k}^{(i)} | x_{m,k} = \alpha_{p}) \prod_{q' \neq q} P(c_{k,q'}^{m} = c_{p,q'})}{\sum_{\alpha_{p}: c_{p,q}=1} P(\hat{x}_{m,k}^{(i)} | x_{m,k} = \alpha_{p}) \prod_{q' \neq q} P(c_{k,q'}^{m} = c_{p,q'})},$$
(18)

where the probability of corresponding coded bits $P(c_{k,q}^m = c_{p,q})$ is obtained from the prior information. The LLRs of coded bits in (18) are deinterleaved and delivered as the input of the soft decoder.

The soft decoder generates extrinsic information, which is fed back to the mapper as the prior information for the next iteration. For the mapper, the probability $P(x_{m,k} = \alpha_p)$ is calculated according to the probability of corresponding coded bits $P(c_{k,q}^m = c_{p,q})$ as

$$P(x_{m,k} = \alpha_p) = \prod_{q=1}^{Q} P(c_{k,q}^m = c_{p,q}),$$

$$(19)$$

where the constellation point $\alpha_p \in \mathcal{S}$ is mapped with Q bits $\mathbf{c}_p = [c_{p,1}, c_{p,2}, \cdots, c_{p,Q}]$. The soft symbols mapped from the (i-1)th iteration of decoder is estimated as the mean of constellation points as

$$\tilde{x}_{m,k}^{(i-1)} = \sum_{\alpha_p \in \mathcal{S}} \alpha_p P(x_{m,k} = \alpha_p). \tag{20}$$

The correlation matrices B and Θ are calculated using the following approximation

$$\beta_m = \theta_m = \frac{1}{K} \sum_{k=1}^K |\tilde{x}_{m,k}^{(i)}|^2, \quad m = 1, 2, \cdots, M,$$
(21)

which is a common assumption in various turbo detection schemes [15]-[17].

The parameters $\check{\mu}_m$ and $\check{\sigma}_m^2$ in the Gaussian distribution $\mathcal{N}(\mu_{m,k}x_{m,k},\sigma_{m,k}^2)$ are calculated using the filter matrices as

$$\check{\mu}_{m} = \frac{1}{K} \sum_{k=1}^{K} \left\{ \mathbf{W}_{k} \mathbf{H}_{k} \right\} [m, m],$$

$$\check{\sigma}_{m}^{2} = \frac{1}{K} \sum_{k=1}^{K} \left\{ \mathbf{\Gamma}_{k} + \mathbf{D}_{k} (\mathbf{B}_{0} - \mathbf{\Theta}_{0}^{H} \mathbf{\Gamma}_{k} \mathbf{\Theta}_{0}) \mathbf{D}_{k}^{H} \right\} [m, m] - \check{\mu}_{m}^{2}.$$
(22)

IV. ITERATIVE CHANNEL ESTIMATION

The accuracy of channel estimation has a significant influence on the performance of UWA communication systems. In the proposed iterative receiver, the channels are estimated at each turbo iteration by utilizing pilots or soft decision symbols, as shown in Fig. 1(b). For the first iteration, pilots inserted before data blocks are used as training signals in channel estimation. After the i-th iteration is completed, soft decision symbols obtained at the previous iteration are fed back to the channel estimator, and served as training signals to update CSI for the (i + 1)-th iteration.

A. MMSE Channel Estimation

In block-wise channel estimation algorithms such as LS and MMSE, the channel is assumed to be quasi-static that the channel is time invariant in one block and varies between different blocks. The training signals from the m-th transmit transducer are denoted as $\{s_{m,k}\}_{k=1}^{K_{\rm tr}}$, and the corresponding received signals at the n-th hydrophone are $\{z_{n,k}\}_{k=1}^{K_{\rm tr}}$, where $K_{\rm tr}$ is the length of training signals. Note that the training signals can be selected as pilots or soft decision symbols in the iterative receiver, and the length $K_{\rm tr}$ is determined by the type of training signals. At the first iteration, pilots with the length K_p are used as training signals with $K_{\rm tr} = K_p$. After the following iteration, soft decision symbols obtained at the previous iteration serve as training signals with $K_{\rm tr} = K$.

By adopting the symbol-rate sampling assumption as in (1), the received signals at the n-th hydrophone corresponding to the training signals are expressed as

$$\mathbf{z}_n = \sum_{m=1}^M \mathbf{S}_m \mathbf{h}_{n,m} + \mathbf{v}_n = \mathbf{S} \mathbf{h}_n + \mathbf{v}_n,$$
 (23)

where $\mathbf{z}_n = [z_{n,1}, z_{n,2}, \cdots, z_{n,K_{\mathrm{tr}}}]^{\mathrm{T}}$ is the received signal vector, and \mathbf{v}_n is the noise vector with normalized noise power σ_0^2 . The channel vector $\mathbf{h}_{n,m} = [h_{n,m}^{(0)}, h_{n,m}^{(1)}, \cdots, h_{n,m}^{(L-1)}]^{\mathrm{T}}$ is corresponding to the subchannel between the m-th transmit transducer and the n-th receive hydrophone, and the concatenated channel vector for the n-th hydrophone is defined as $\mathbf{h}_n = [\mathbf{h}_{n,1}^{\mathrm{T}}, \mathbf{h}_{n,2}^{\mathrm{T}}, \cdots, \mathbf{h}_{n,M}^{\mathrm{T}}]^{\mathrm{T}}$. The training signals from the m-th transducer form a matrix defined as

$$\mathbf{S}_{m} = \begin{bmatrix} s_{m,1} & 0 & \cdots & 0 \\ s_{m,2} & s_{m,1} & \cdots & 0 \\ \vdots & \vdots & \ddots & \vdots \\ s_{m,L} & s_{m,L-1} & \cdots & s_{m,1} \\ \vdots & \vdots & \ddots & \vdots \\ s_{m,K_{tr}} & s_{m,K_{tr}-1} & \cdots & s_{m,K_{tr}-L+1} \end{bmatrix},$$
(24)

and the matrix for the whole training signals is denoted as $\mathbf{S} = [\mathbf{S}_1, \mathbf{S}_2, \cdots, \mathbf{S}_M]$.

By considering the effect of noise, the CIR is estimated using the MMSE algorithm as [24]

$$\hat{\mathbf{h}}_n^{\text{MMSE}} = \left(\mathbf{S}^{\text{H}}\mathbf{S} + \sigma_0^2 \mathbf{I}_{LM}\right)^{-1} \mathbf{S}^{\text{H}} \mathbf{z}_n. \tag{25}$$

Since matrix inversion is adopted in the MMSE channel estimation, the computational complexity of the block-wise algorithm is prohibitively high, especially for matrices with large size.

B. NLMS Channel Estimation

In fast time-varying channels, the quasi-static channel assumption adopted in the block-wise algorithm is inapplicable and suffers from performance degradation [28]. Compared with the block-wise algorithms, symbol-wise adaptive algorithms can estimate the channel coefficients with low computational complexity due to no matrix inversion. Channel estimation performed by symbol-wise adaptive algorithms have been applied to UWA communications to reduce the complexity and track the time variation of the UWA channels [30]. However, symbol-wise adaptive algorithms require long training signals to overcome slow convergence. The method of data reuse is commonly adopted to reduce the overhead of training signals, that a short training signal is reused for several times with decreasing step sizes in the adaptive algorithms.

In the NLMS algorithm, the *L*-tap adaptive filter $\hat{\mathbf{h}}_{n,m}(k) = [\hat{h}_{n,m}^{(0)}(k), \hat{h}_{n,m}^{(1)}(k), \cdots, \hat{h}_{n,m}^{(L-1)}(k)]^{\mathrm{T}}$ is utilized to model the subchannel between the *m*-th transducer and the *n*-th hydrophone, and the input

vector of this adaptive filter is obtained from training signals as $\mathbf{s}_m(k) = [s_{m,k}, s_{m,k-1}, \cdots, s_{m,k-L+1}]^{\mathrm{T}}$, where k is the index of time instants. By combining the M branches into a joint structure, the concatenated adaptive filter and input vector are denoted as $\hat{\mathbf{h}}_n(k) = [\hat{\mathbf{h}}_{n,1}(k)^{\mathrm{T}}, \hat{\mathbf{h}}_{n,2}(k)^{\mathrm{T}}, \cdots, \hat{\mathbf{h}}_{n,M}(k)^{\mathrm{T}}]^{\mathrm{T}}$ and $\mathbf{s}(k) = [\mathbf{s}_1(k)^{\mathrm{T}}, \mathbf{s}_2(k)^{\mathrm{T}}, \cdots, \mathbf{s}_M(k)^{\mathrm{T}}]^{\mathrm{T}}$, respectively. The error between the filter output and the actual received signal is calculated as $e(k) = z_{n,k} - \mathbf{s}(k)^{\mathrm{H}} \hat{\mathbf{h}}_n(k)$, which is utilized to update the filter coefficients. The time-varying channel is modeled by the adaptive filter as

$$\hat{\mathbf{h}}_n(k+1) = \hat{\mathbf{h}}_n(k) + \mu(k) \frac{e^*(k)}{\delta + \mathbf{s}(k)^{\mathrm{H}} \mathbf{s}(k)} \mathbf{s}(k), \tag{26}$$

where δ is a small positive parameter to avoid possible division by zero. The step size $\mu(k)$ determines the convergence rate and steady-state errors. During the date reuse, the step size is initially set as $\mu(k)=1$ to ensure a fast convergence rate, and then decreases for the subsequent reuse to achieve a low steady-state error.

The NLMS algorithms is performed at each iteration to re-estimate the channel during the process of turbo equalization. The input of adaptive filter is obtained from pilots at the first iteration. After the i-th iteration is completed, soft decision symbols will be fed back to the channel estimator as training signals for the (i+1)-th iteration. It is noted that the last updated CIR in the symbol-wise channel estimation is delivered to the block-wise frequency domain equalization. Since the training signal is reused for several times during the adaptive algorithm, the last updated CIR has approximately converged to the stable state.

V. COMPUTATIONAL COMPLEXITY ANALYSIS

Computational complexity of the proposed iterative receiver is analyzed in this section. Detailed values of complexity for different turbo equalization schemes and channel estimation algorithms will be presented in the following two subsections, respectively. Here the complexity of the size-K FFT is approximated as $\frac{K}{2}\log_2 K$, and the complexity of matrix inversion with size $M\times M$ is approximated as $\frac{M^3}{2}$ [32].

A. Complexity of Turbo Equalization

We compare turbo equalization schemes conducted in the frequency domain and in the time domain. The FDE-FDDF scheme is performed in the frequency domain by utilized a feedforward filter and a feedback filter, as mentioned in Section III.B. The TDE-PIC scheme is performed in the time domain by subtracting *a priori* mean of the interfering symbols from the received signals, where the ISI and CCI are reconstructed using decoder outputs of the previous iteration and then removed in parallel simultaneously [10]. Computational complexity of the FDE-FDDF scheme and the TDE-PIC scheme for a data block is approximated as in Table I. In the FDE-FDDF scheme, channel matrix **H**, correlation matrices **B**

and Θ are all block diagonal matrices. Consequently, the feedforward and the feedback matrices in the FDE-FDDF scheme are calculated by each submatrix, which reduces the complexity from $O(\{KN\}^3)$ to $O(KN^3)$. Here we give detailed values of the two turbo equalization schemes. Using the parameters of the 2×12 MIMO system described in Section VI, detailed values of expressions in Table I are calculated to illustrate the low complexity of frequency domain turbo equalization. The overall complexity of the FDE-FDDF scheme is reduced by three orders of magnitude than the TDE-PIC scheme. The low complexity of FDTE makes it a potential alternative to be applied to real-time processing platforms in UWA communications.

TABLE I $\mbox{Complexity of turbo equalization schemes for a data block } (M=2,\,N=12,\,K=1024,\,K_f=121).$

Operation	FDE-FDI)F	TDE-PIC		
	Complexity	Detailed Value	Complexity	Detailed Values	
Filter Design	$O(KN^3)$	1.77×10^{6}	$O(K_{\mathrm{f}}^3 N^3)$	3.06×10^{9}	
Filtering	$KM\{M+N\}$	2.87×10^4	$K_{ m f}KMN$	2.97×10^6	
FFT	$\frac{K}{2}\{2M+N\}\log_2 K$	8.19×10^4	N/A	0	
Total		1.88×10^{6}		3.06×10^{9}	

 ${\it TABLE~II}$ Complexity of Channel estimation algorithms for a data block ($M=2,\,N=12,\,K=1024,\,\gamma=5$).

Channel Estimation	Complexity	Detailed Values		
Channel Estimation	Complexity	$K_{\rm tr} = 240$	$K_{\rm tr} = 1024$	
MMSE	$(LM)^3 + (LM)^2(K_{\rm tr} + N) + LMK_{\rm tr}N$	8.96×10^{6}	3.05×10^{7}	
NLMS	$K_{\mathrm{tr}}N[LM(2\gamma+1)+2\gamma]$	5.10×10^6	2.17×10^7	

B. Complexity of Channel Estimation

The two channel estimation algorithms adopted in the iterative receiver is analyzed. Computational complexity of the MMSE algorithm and the NLMS algorithm for a data block is approximated as in Table II. The number of data reuse rounds in the NLMS algorithm is set as $\gamma=5$. Compared with the block-wise MMSE algorithm, the symbol-wise NLMS algorithm can estimate channel coefficients with much lower computational complexity. On the other hand, the NLMS algorithm suffers a slight

degradation of estimation accuracy in our experiment results of SPACE08, which will be demonstrated in Section VI. As a result, the NLMS channel estimation algorithm is a good choice for turbo equalization to achieve complexity-performance tradeoff.

VI. EXPERIMENTAL RESULTS OF SPACE08

A. Overview of the SPACE08 Experiment

The proposed iterative receiver has been adopted to process undersea experimental data collected during the SPACE08 experiment. This experiment was conducted off the coast of Martha's Vineyard, Edgartown, MA in October, 2008. During the experiment, the water depth was approximately 15 m, and the communication distance could be set as 60 m, 200 m, or 1000 m. There were four transducers at the transmitter and twelve hydrophones at the receiver. The number of active transducers could be configured to launch different transmissions. Our transmission was designed as a 2×12 SC-MIMO system with communication distance 1000 m. The symbol interval was $T_{\rm s} = 0.1024$ ms, and the carrier frequency was $f_{\rm c} = 13$ kHz. Input bits were encoded by a rate-1/2 convolutional channel encoder with generator polynomial $[G_1, G_2] = [17, 13]_{\rm oct}$. The transmission frame structure is illustrated in Fig. 2. Linear frequency modulation (LFM) signals added before and after the data payload were utilized to estimate the carrier frequency offset and perform coarse timing synchronization. Precise timing synchronization was conducted by using the maximum length sequence termed as the m-sequence. The length of data block was chosen as K = 1024. Gaps with length $K_{\rm g} = 120$ were inserted between data block and pilots to avoid inter-block interference. Data symbols with QPSK, 8PSK and 16QAM were transmitted in blocks. For each modulation, 240 available blocks were collected during the experiment.

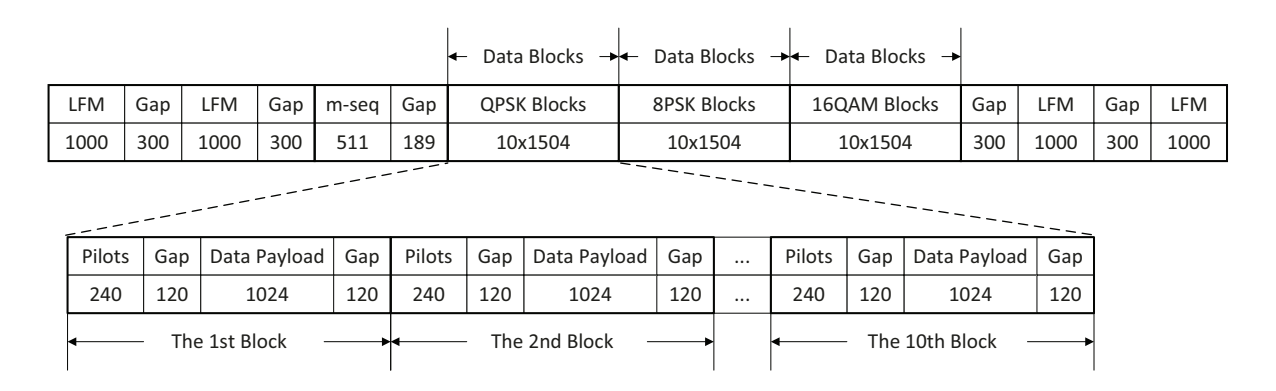


Fig. 2. Data structure in the SPACE08 experiment.

The received signals at the first hydrophone of the Packet 3012354F009-C0-S5 are demonstrated as an example in Fig. 3. The amplitude and the spectrogram of the passband signals are shown in top subfigure

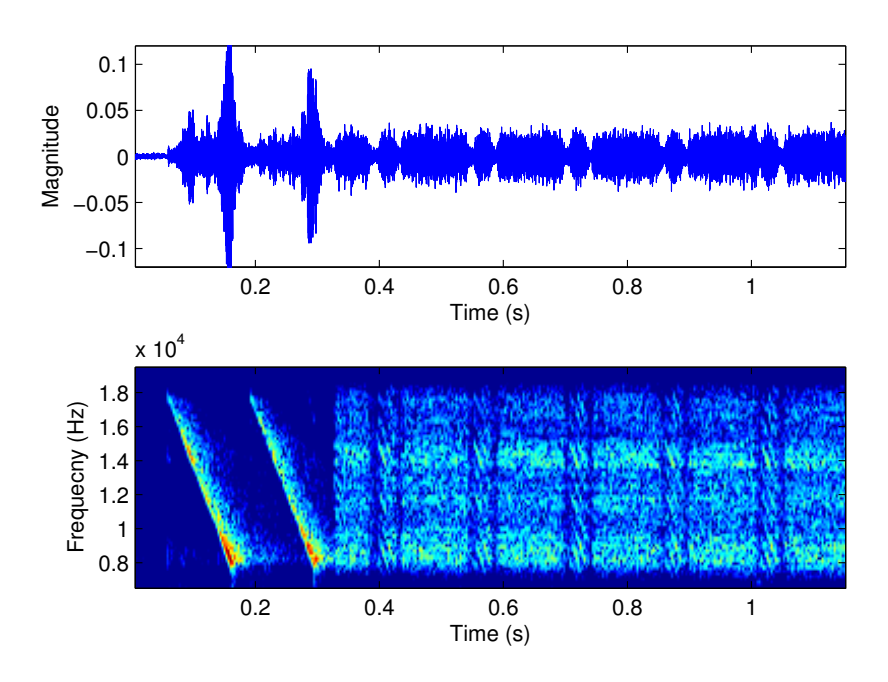


Fig. 3. Received passband signals in Packet 3012354F009-C0-S5-1. (a) Magnitude of the received signals. (b) Spectrogram of the received signals.

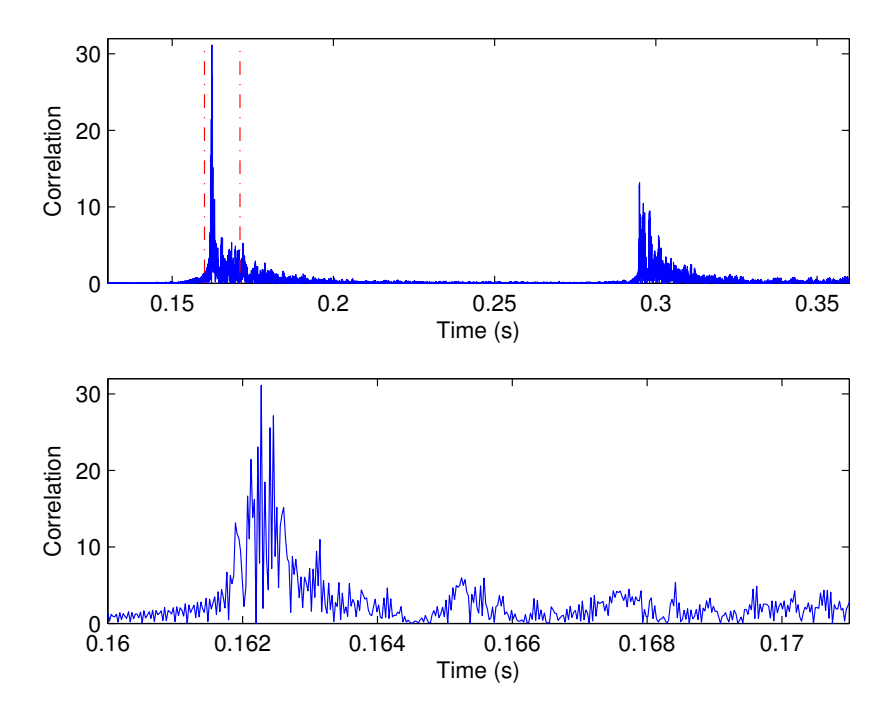


Fig. 4. Correlation results of local LFM signals and received signals in Packet 3012354F009-C0-S5. (a) Correlation results of the received signals. (b) Enlarged correlation results from (a).

and the bottom subfigure, respectively. Based on the data structure depicted in Fig. 2, we can clearly observe the LFM signals, m-sequence, pilots and data blocks in Fig. 3. The LFM signals are adopted in synchronization to estimate the beginning of received signals. Correlation results of local LFM signals and received signals at the first hydrophone are demonstrated in Fig. 4. Two clusters of correlation peaks are observed in the top subfigure, corresponding to the two LFM signals. The bottom subfigure shows the zoomed correlation results, which can be utilized to coarsely estimate the length of underwater acoustic channels. In the case shown in Fig. 4, the channel length is less than 10 ms. The delay spread of the 1000 m transmission in SPACE08 was estimated as 8.2 ms [18]. Consequently, we set the length of underwater acoustic channels as 80 taps.

B. Accuracy of Channel Estimation Algorithms

In the proposed receiver, iterative channel estimation is performed to improve the accuracy of CSI estimation. At the initial iteration, pilots inserted before the data blocks are utilized as training signals. At the following iterations, soft decision symbols obtained at the previous iteration are fed back to the channel estimator and served as training signals to re-estimate the UWA channels. Examples of the channel estimation results in Packet 3011754F009-C0-S5 are shown in Fig. 5 to demonstrate the characteristics of UWA channels. In this packet, the CIRs of the first transducer have higher power levels than those of the second transducer, which leads to better transmission performance for the first transducer. The unbalanced multipath channels make it more challenging to recover the transmitted bits.

The channel estimation results using iterative channel estimation are demonstrated in Fig. 6. Magnitudes and phases of the estimated CIRs are shown in the top subfigure and the bottom subfigure, respectively. Since the exact CIR is unavailable in the experiment, we use all transmitted symbols in the data block as training signals to estimate the approximated CSI $\dot{\mathbf{h}}$, which will be treated as the actual CIR. As the iteration progresses, the estimated CIR get closer to the actual one. To quantitatively evaluate the performance of these channel estimation methods, the relative error of CSI estimation is defined as

$$e_{\mathbf{h}} = \frac{||\dot{\mathbf{h}} - \hat{\mathbf{h}}||}{||\dot{\mathbf{h}}||},\tag{27}$$

where $\hat{\mathbf{h}}$ is the estimated CSI using one of the mentioned channel estimation methods, and $||\mathbf{h}||$ is the Euclidean norm of the vector \mathbf{h} .

Relative errors of the two iterative channel estimation methods (MMSE-ICE and NLMS-ICE) in frequency domain turbo equalization are demonstrated in Table III. Relative errors of channel estimation at the first iteration are extremely large, which means that the estimated CSI is unreliable to guarantee the performance. Due to the rapid time variation of UWA channels, the estimated CSIs using pilots are

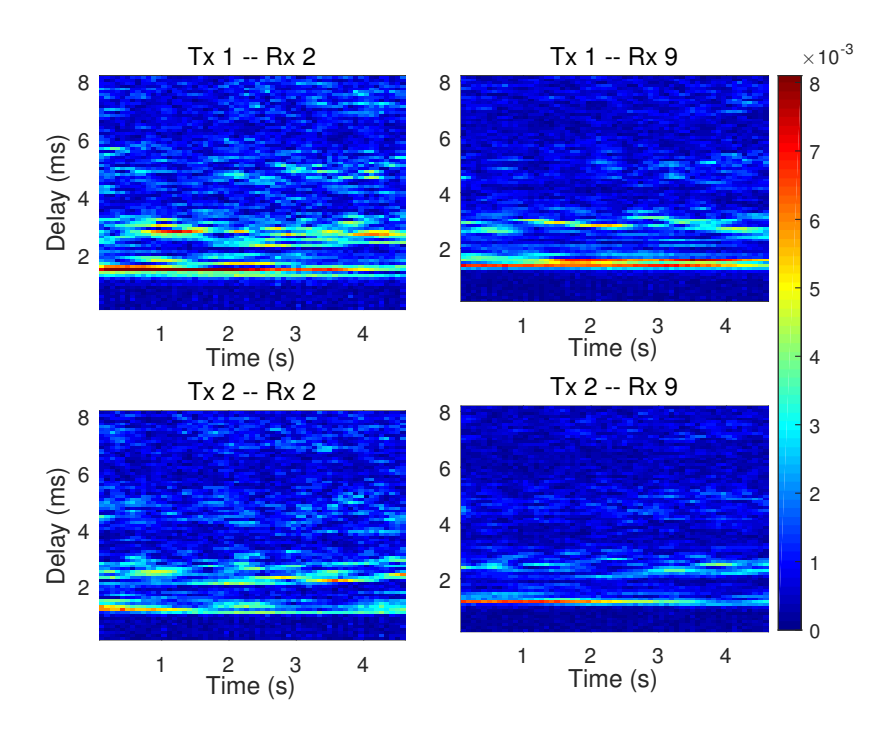
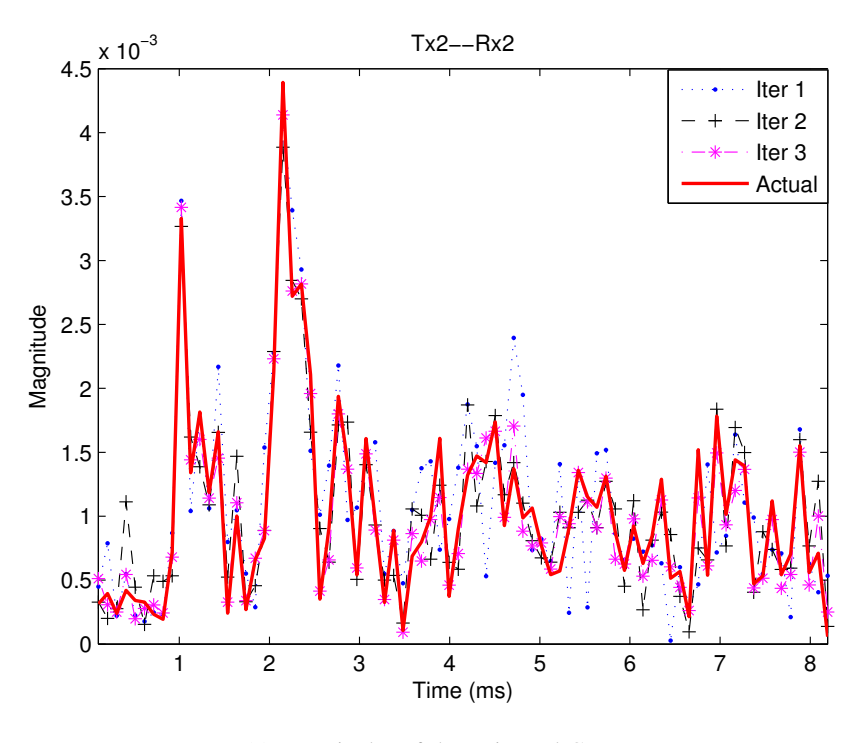


Fig. 5. Magnitudes and delays of the time-varying channel impulse responses in Packet 3012354F009-C0-S5. The transmission distance is 1000 m. The MMSE algorithm is adopted in the iterative channel estimation.

obviously different from the instantaneous channels through which the data block is transmitted. At the following iterations, soft decision symbols are utilized as training signals to re-estimate the channels. As the iteration progresses, the relative errors degrade rapidly. As a result, iterative channel estimation is an effective method to improve the estimation accuracy of time-varying UWA channels. Comparing the effect of different modulations, the estimated CSI using QPSK is more accurate than 8PSK and 16QAM. Due to the low order of modulation, soft decision symbols of QPSK are more reliable during the iterative process, which can also be verified by bit error rate (BER) performance in the next subsection.

Compared with the block-wise MMSE channel estimation algorithm, the symbol-wise NLMS algorithm suffers slight degradation of estimation accuracy, which is different from the results of other experiments [28], [30]. The possible reason is that our experiment adopted the block transmission instead of the burst structure, and the block-wise frequency domain turbo equalization is utilized in the data processing. The quasi-static channel assumption that the UWA channel is time invariant in one block is adopted for block-wise frequency domain equalization to reduce the complexity. Although the symbol-wise adaptive algorithms can update the channel coefficients dynamically, the estimated instantaneous CIR is delivered to the block-wise equalizer which requires the quasi-static CIR as the input.



(a) Magnitudes of the estimated CIRs

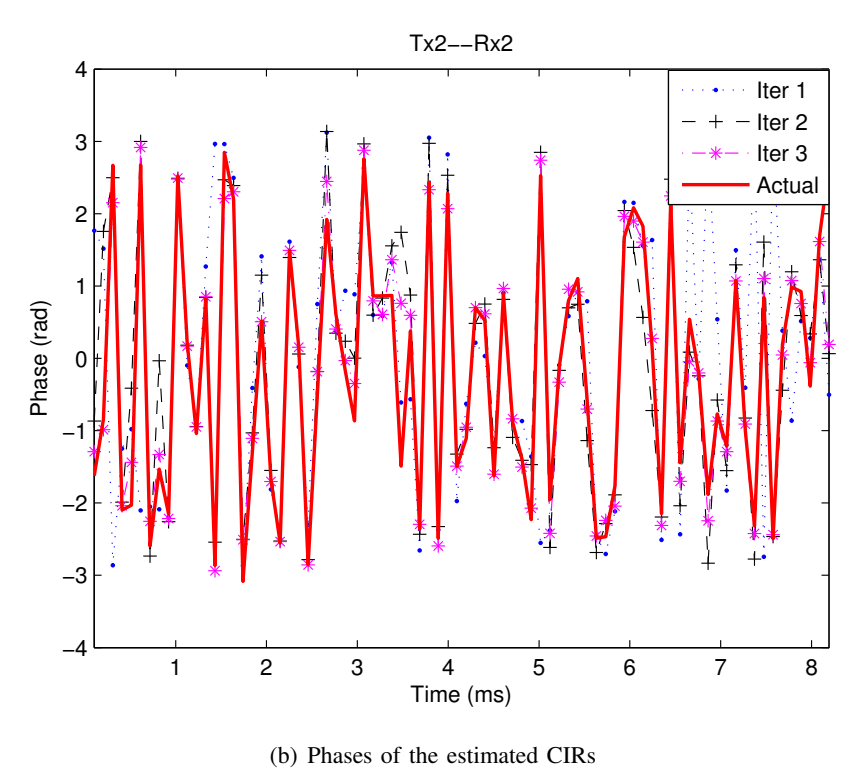


Fig. 6. The estimated CIRs using iterative channel estimation between the second transducer and the second hydrophone in Packet 3012354F009-C0-S5. Four iterations are conducted using the FDE-FDDF scheme. The MMSE algorithm is adopted in the iterative channel estimation.

TABLE III RELATIVE ERRORS OF ITERATIVE CHANNEL ESTIMATION METHODS USING MMSE AND NLMS IN PACKET 3012354F009-C0-S5.

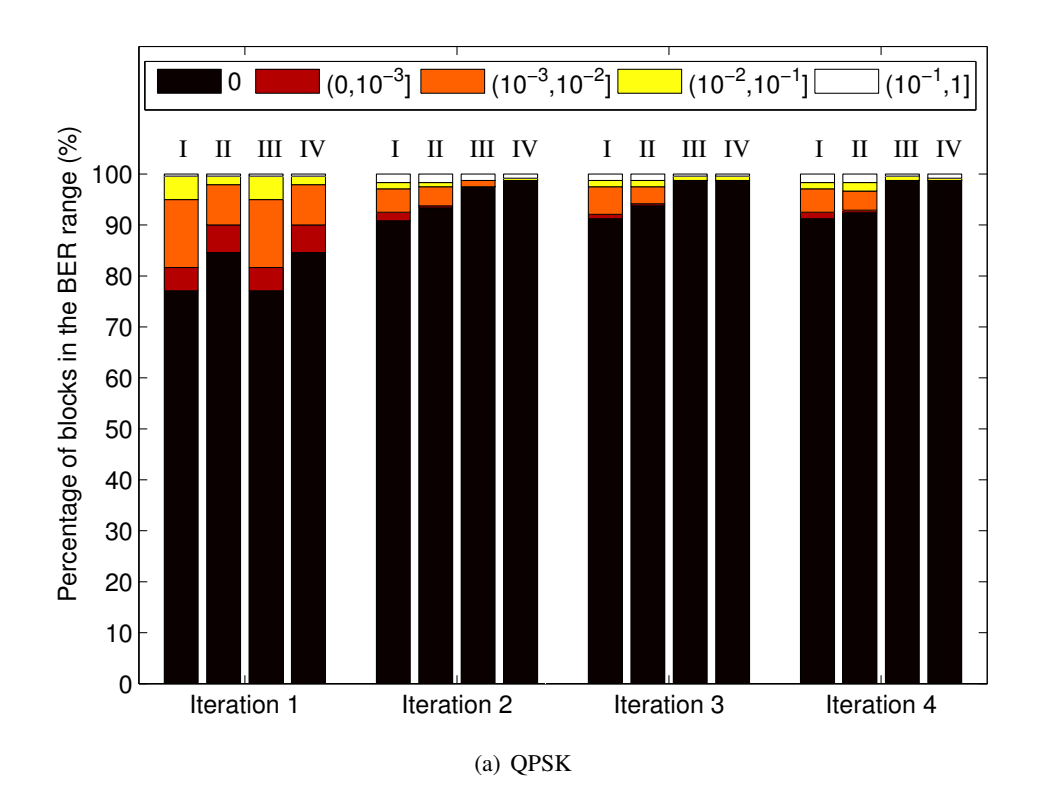
T44'	QPSK		8PSK		16QAM	
Iteration	MMSE	NLMS	MMSE	NLMS	MMSE	NLMS
Iteration 1	0.339	0.378	0.403	0.444	0.435	0.475
Iteration 2	0	0	0.098	0.144	0.212	0.245
Iteration 3	0	0	0.015	0.028	0.143	0.170
Iteration 4	0	0	0	0	0.095	0.126

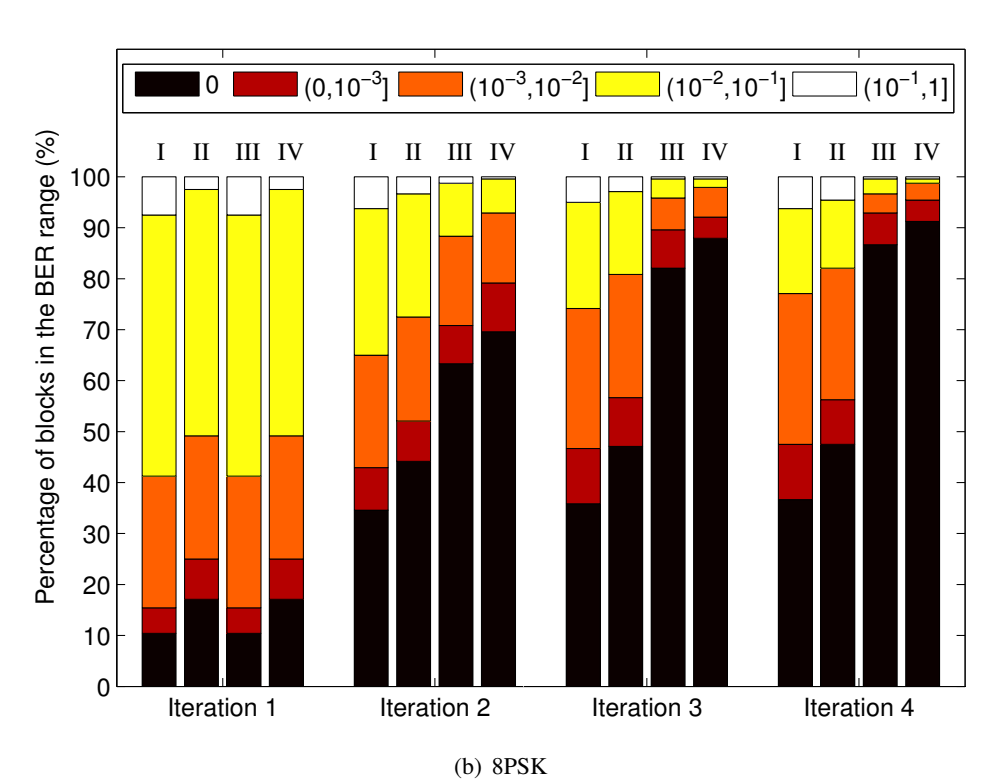
C. Bit Error Rate Performance

Received data blocks are processed by frequency domain turbo equalization using four channel estimation methods. MMSE algorithm and NLMS algorithm are adopted in the iterative channel estimation as MMSE-ICE and NLMS-ICE, thus channel coefficients are updated at each iteration in these two schemes. Two non-iterative channel estimation methods (MMSE-NCE and NLMS-NCE) are also performed to illustrate the advantage of iterative channel estimation. Four iterations are conducted for each scheme.

TABLE IV BER Results after Four Iterations, Using Time Domain Turbo Equalization with Non-iterative Channel Estimation (NCE) or Iterative Channel Estimation (ICE).

Iteration	Iterative	Channel	Percentage of the packets that fall into the BER range (%)				
	scheme	estimation	BER = 0	$(0, 10^{-3}]$	$(10^{-3}, 10^{-2}]$	$(10^{-2}, 10^{-1}]$	$(10^{-1}, 1]$
QPSK -	NCE	NLMS	91.25	1.25	4.58	1.25	1.67
		MMSE	92.50	0.42	3.75	1.67	1.67
	ICE	NLMS	98.75	0.00	0.00	0.83	0.42
		MMSE	98.75	0.00	0.00	0.42	0.83
8PSK	NCE	NLMS	36.67	10.83	29.58	16.67	6.25
		MMSE	47.50	8.75	25.83	13.33	4.58
	ICE	NLMS	86.67	6.25	3.75	2.92	0.42
		MMSE	91.25	4.17	3.33	0.83	0.42
16QAM	NCE	NLMS	10.00	2.50	23.33	31.25	32.92
		MMSE	13.75	7.92	24.17	24.58	29.58
	ICE	NLMS	42.92	7.92	15.83	20.83	12.50
		MMSE	44.58	10.00	15.83	19.17	10.42





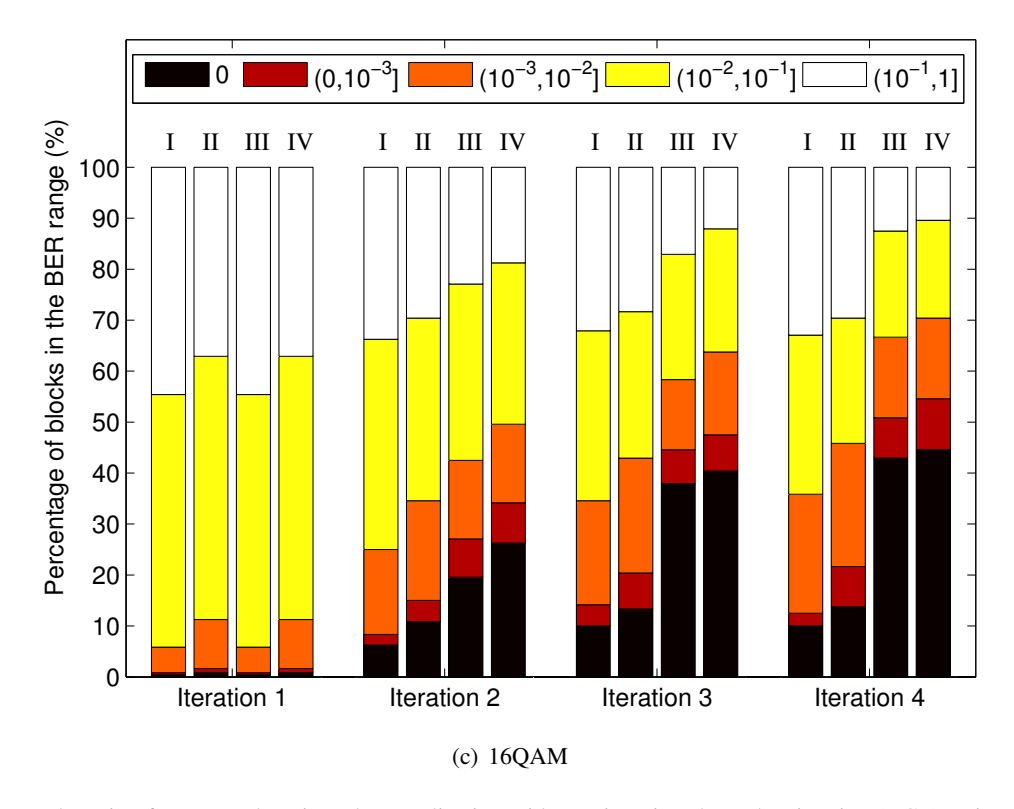


Fig. 7. BER results using frequency domain turbo equalization with non-iterative channel estimation (NCE) or iterative channel estimation (ICE). Four channel estimation methods are adopted in the iterative receiver. (I) NLMS algorithm with NCE, (II) MMSE algorithm with NCE, (III) NLMS algorithm with ICE, and (IV) MMSE algorithm with ICE.

Experimental data processing results are demonstrated in Fig. 7, in terms of the percentage of blocks falling into the specified BER ranges. As shown in Fig. 7(a), the majority of QPSK data blocks achieve zero BER after four iterations. At the initial iteration, pilots are utilized to estimate CSI for all schemes. In the later iterations, the CSI is not updated in non-iterative channel estimation methods (MMSE-NCE and NLMS-NCE). However, in iterative channel estimation methods (MMSE-ICE and NLMS-ICE), soft decision symbols obtained at the previous iteration are used as training signals to update CSI for the current iteration, which improves the accuracy of channel estimation. In the view of BER results, the performance of frequency domain turbo equalizations with iterative channel estimation outperforms those with non-iterative channel estimation. As the iteration progresses, the advantage of iterative channel estimation is more obvious. Compared with MMSE-ICE, NLMS-ICE can estimate CSI with low computational complexity at a cost of slightly inferior BER performance.

BER results of 8PSK and 16QAM are demonstrated in Fig. 7(b) and Fig. 7(c), respectively. With the increase of iterations, the number of bit errors degrades rapidly. After four iterations of frequency domain turbo equalization with iterative channel estimation, about 90% of 8PSK data blocks achieve

zero BER, and over 40% of 16QAM data blocks achieve zero BER. The performance of 16QAM is much worse than that of QPSK because of the high order of modulation. Using frequency domain turbo equalization, the BER results of 16QAM have been improved significantly after four iterations. Compared with the non-iterative channel estimation methods, the iterative channel estimation methods achieve much better performance, because soft decision symbols are utilized as training signals to reestimate the UWA channels at each iteration. As the number of iteration increases, the advantage of iterative channel estimation is more obvious.

Time domain turbo equalization is also included to compare with frequency domain turbo equalization. The four channel estimation methods mentioned above are also combined with the TDE-PIC scheme. Each time domain turbo equalization scheme is conducted for four iterations. For the time domain filter in the TDE-PIC scheme, the length of causal part is set as 80, and the length of anti-causal part is set as 40. As a result, the total filter length is set as $K_f = 80 + 1 + 40 = 121$. The BER results after four iterations using different channel estimation methods are demonstrated in Table IV. Compared with frequency domain turbo equalization, time domain turbo equalization achieves slightly better BER performance. However, the computational complexity of time domain turbo equalization is prohibitively high, especially in UWA channels with long delay spread.

Constellation diagrams are often utilized to check the reliability of the recovered symbols. The equalized symbols and soft decision symbols in frequency domain turbo equalization with MMSE-ICE are shown in Fig. 8 and Fig. 9, respectively. Symbols of QPSK, 8PSK and 16QAM during the four iterations are demonstrated in the three rows. The soft decision symbols converge to the ideal constellation points during the iterations, while equalized symbols are improved slightly. In the view of constellation diagram, soft decision symbols are more reliable than equalized symbols due to the usage of soft decoder. Extrinsic information is generated by the soft decoder, and then fed back as the prior information for the next iteration. By exchanging soft information between the equalizer and the soft decoder iteratively, frequency domain turbo equalization is an effective method to improve the performance of MIMO systems in UWA channels.

VII. CONCLUSION

In this paper, an iterative receiver is proposed for SC-MIMO UWA communications, by combining frequency domain turbo equalization with iterative channel estimation. Soft decision symbols are not only fed back to the equalizer to cancel the ISI and CCI, but also used as training signals in the channel estimator to re-estimate the UWA channels. Compared with time domain turbo equalization, frequency domain turbo equalization reduces the complexity significantly, while comparable performance

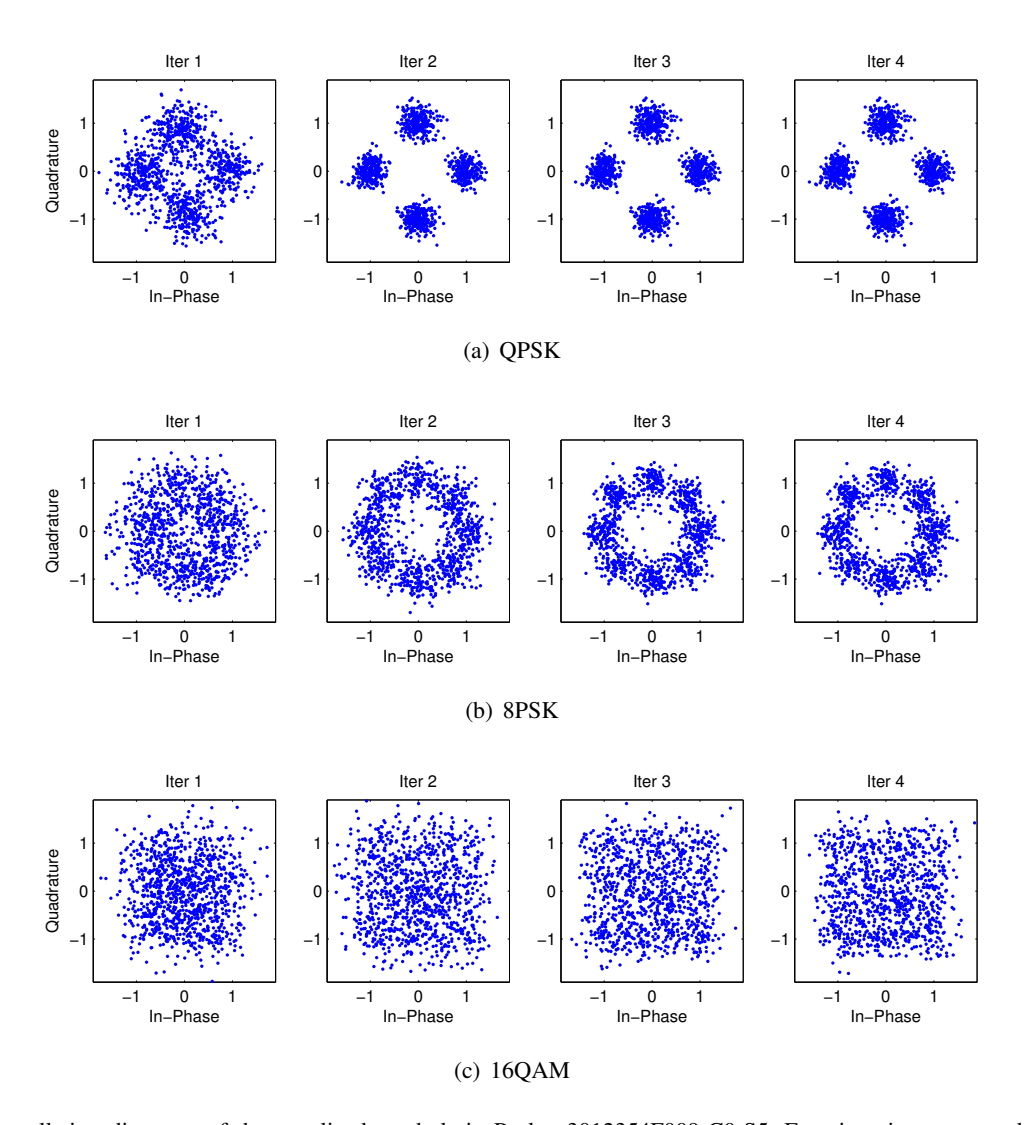


Fig. 8. Constellation diagrams of the equalized symbols in Packet 3012354F009-C0-S5. Four iterations are conducted using the FDE-FDDF scheme. The MMSE algorithm is adopted in the iterative channel estimation.

is achieved. Using pilots at the first iteration and soft decision symbols in the following iterations, iterative channel estimation further improves the accuracy of the estimated CSI. The proposed iterative receiver has been verified through undersea experimental data collected in SPACE08.

ACKNOWLEDGMENT

This work is supported in part by the Beijing Higher Education Young Elite Teacher Project (Grant No. YETP0101), the National Science Foundation of China (Grant No. 61471221) and the U.S. National Science Foundation (Grant No. ECCS-1408316). This work had been carried out while Z. Chen was a visiting scholar at Missouri University of Science and Technology.

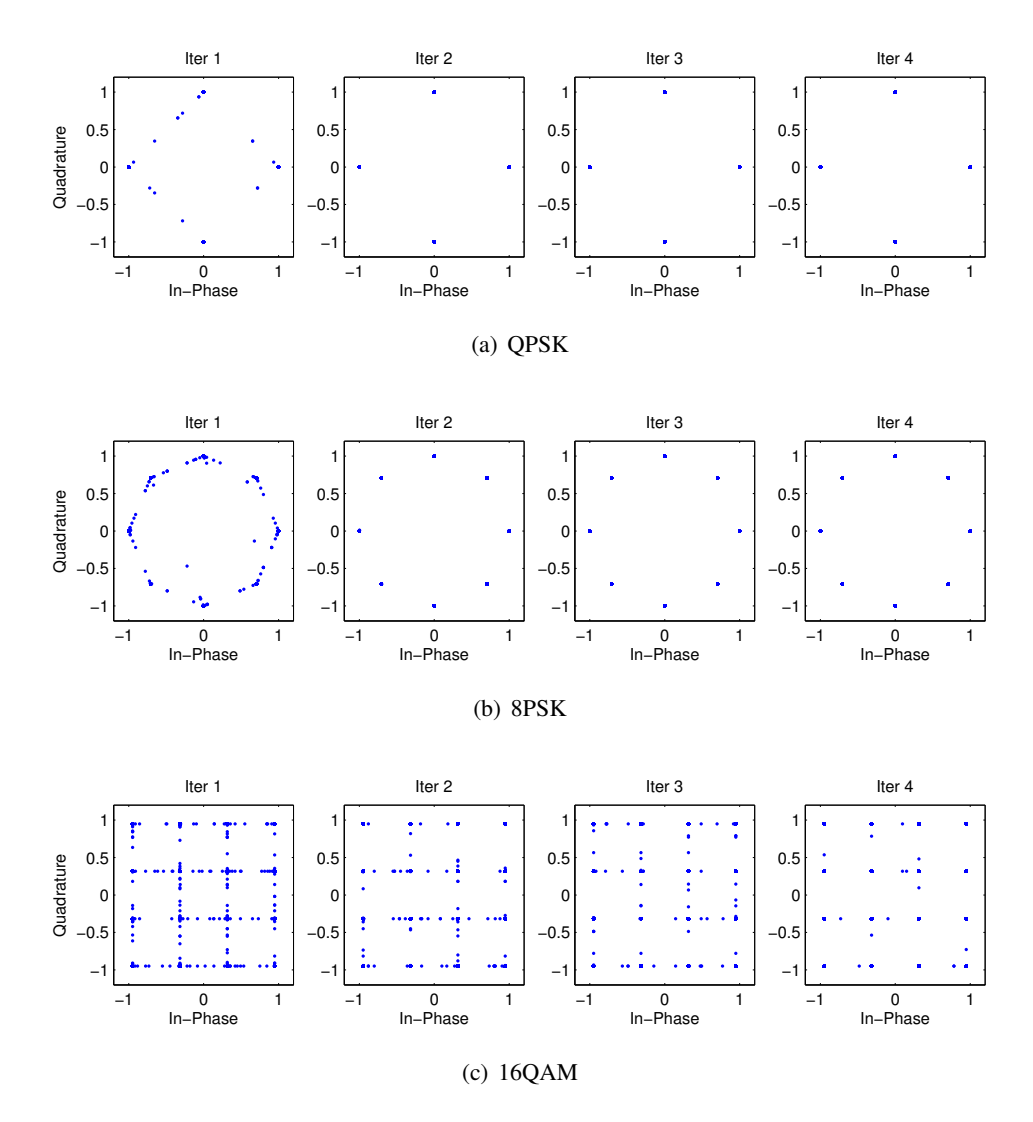


Fig. 9. Constellation diagrams of soft decision symbols in Packet 3012354F009-C0-S5. Four iterations are conducted using the FDE-FDDF scheme. The MMSE algorithm is adopted in the iterative channel estimation.

REFERENCES

- [1] Z. Chen, Y. R. Zheng, J. Wang, and J. Song, "Frequency domain turbo equalization with iterative channel estimation for single carrier MIMO underwater acoustic communications," in *IEEE VTC Fall 2015*, Sep. 2015, pp. 1–5.
- [2] M. Stojanovic and J. Preisig, "Underwater acoustic communication channels: Propagation models and statistical characterization," *IEEE Commun. Mag.*, vol. 47, no. 1, pp. 84–89, Jan. 2009.
- [3] A. C. Singer, J. K. Nelson, and S. S. Kozat, "Signal processing for underwater acoustic communications," *IEEE Commun. Mag.*, vol. 47, no. 1, pp. 90–96, 2009.
- [4] B. Li, S. Zhou, M. Stojanovic, L. Freitag, and P. Willett, "Multicarrier communication over underwater acoustic channels with nonuniform Doppler shifts," *IEEE J. Ocean. Eng.*, vol. 33, no. 2, pp. 198–209, 2008.
- [5] Y. V. Zakharov and A. K. Morozov, "OFDM transmission without guard interval in fast-varying underwater acoustic channels," *IEEE J. Ocean. Eng.*, vol. 40, no. 1, pp. 144–158, 2015.

- [6] J. Zhang and Y. R. Zheng, "Bandwidth-efficient frequency-domain equalization for single carrier multiple-input multiple-output underwater acoustic communications," J. Acoustic Society America, vol. 128, no. 5, pp. 2910–2919, 2010.
- [7] M. Xia, D. Rouseff, J. A. Ritcey, X. Zou, C. Polprasert, and W. Xu, "Underwater acoustic communication in a highly refractive environment using SC-FDE," *IEEE J. Ocean. Eng.*, vol. 39, no. 3, pp. 491–499, 2014.
- [8] N. Benvenuto, R. Dinis, D. Falconer, and S. Tomasin, "Single carrier modulation with nonlinear frequency domain equalization: an idea whose time has come—again," *Proc. IEEE*, vol. 98, no. 1, pp. 69–96, 2010.
- [9] M. Tuchler, A. C. Singer, and R. Koetter, "Minimum mean squared error equalization using a priori information," *IEEE Trans. Signal Process.*, vol. 50, no. 3, pp. 673–683, 2002.
- [10] J. Tao, J. Wu, Y. R. Zheng, and C. Xiao, "Enhanced MIMO LMMSE turbo equalization: algorithm, simulations, and undersea experimental results," *IEEE Trans. Signal Process.*, vol. 59, no. 8, pp. 3813–3823, 2011.
- [11] R. R. Lopes and J. R. Barry, "The soft-feedback equalizer for turbo equalization of highly dispersive channels," *IEEE Trans. Commun.*, vol. 54, no. 5, pp. 783–788, 2006.
- [12] H. Lou and C. Xiao, "Soft-decision feedback turbo equalization for multilevel modulations," *IEEE Trans. Signal Process.*, vol. 59, no. 1, pp. 186–195, 2011.
- [13] M. Tuchler and J. Hagenauer, "Linear time and frequency domain turbo equalization," in *Proc. IEEE VTC Spring 2001*, vol. 2, May 2001, pp. 1449–1453.
- [14] N. Benvenuto and S. Tomasin, "Iterative design and detection of a DFE in the frequency domain," *IEEE Trans. Commun.*, vol. 53, no. 11, pp. 1867–1875, 2005.
- [15] B. Ng, C.-T. Lam, and D. Falconer, "Turbo frequency domain equalization for single-carrier broadband wireless systems," *IEEE Trans. Wireless Commun.*, vol. 6, no. 2, pp. 759–767, 2007.
- [16] C. Zhang, Z. Wang, C. Pan, S. Chen, and L. Hanzo, "Low-complexity iterative frequency domain decision feedback equalization," *IEEE Trans. Veh. Technol.*, vol. 60, no. 3, pp. 1295–1301, 2011.
- [17] G. M. Guvensen and A. Ozgur Yilmaz, "A general framework for optimum iterative blockwise equalization of single carrier MIMO systems and asymptotic performance analysis," *IEEE Trans. Commun.*, vol. 61, no. 2, pp. 609–619, 2013.
- [18] J. Zhang and Y. R. Zheng, "Frequency-domain turbo equalization with soft successive interference cancellation for single carrier MIMO underwater acoustic communications," *IEEE Trans. Wireless Commun.*, vol. 10, no. 9, pp. 2872–2882, 2011.
- [19] J. Tao, "Single-carrier frequency-domain turbo equalization with various soft interference cancellation schemes for MIMO systems," *IEEE Trans. Commun.*, vol. 63, no. 9, pp. 3206–3217, 2015.
- [20] L. Wang, J. Tao, and Y. R. Zheng, "Single-carrier frequency-domain turbo equalization without cyclic prefix or zero padding for underwater acoustic communications," *J. Acoustic Society America*, vol. 132, no. 6, pp. 3809–3817, 2012.
- [21] A. Rafati, H. Lou, and C. Xiao, "Soft-decision feedback turbo equalization for LDPC-coded MIMO underwater acoustic communications," *IEEE J. Ocean. Eng.*, vol. 39, no. 1, pp. 90–99, 2014.
- [22] W. Duan and Y. R. Zheng, "Bidirectional soft-decision feedback equalization for robust MIMO underwater acoustic communications," in *MTS/IEEE OCEANS '14*, St. John's, Sept. 2014, pp. 1–6.
- [23] Y. R. Zheng, J. Wu, and C. Xiao, "Turbo equalization for single-carrier underwater acoustic communications," *IEEE Commun. Mag.*, vol. 53, no. 11, pp. 79–87, 2015.
- [24] M. Biguesh and A. B. Gershman, "Training-based MIMO channel estimation: a study of estimator tradeoffs and optimal training signals," *IEEE Trans. Signal Process.*, vol. 54, no. 3, pp. 884–893, 2006.
- [25] C. R. Berger, S. Zhou, J. C. Preisig, and P. Willett, "Sparse channel estimation for multicarrier underwater acoustic communication: From subspace methods to compressed sensing," *IEEE Trans. Signal Process.*, vol. 58, no. 3, pp. 1708– 1721, 2010.

- [26] Z. Wang, S. Zhou, J. C. Preisig, K. R. Pattipati, and P. Willett, "Clustered adaptation for estimation of time-varying underwater acoustic channels," *IEEE Trans. Signal Process.*, vol. 60, no. 6, pp. 3079–3091, 2012.
- [27] F. Qu, X. Nie, and W. Xu, "A two-stage approach for the estimation of doubly spread acoustic channels," *IEEE J. Ocean. Eng.*, vol. 40, no. 1, pp. 131–143, 2015.
- [28] K. Pelekanakis and M. Chitre, "New sparse adaptive algorithms based on the natural gradient and the L0-norm," *IEEE J. Ocean. Eng.*, vol. 38, no. 2, pp. 323–332, 2013.
- [29] D. Yoon and J. Moon, "Low-complexity iterative channel estimation for turbo receivers," *IEEE Trans. Commun.*, vol. 60, no. 5, pp. 1182–1187, 2012.
- [30] Z. Yang and Y. R. Zheng, "Iterative channel estimation and turbo equalization for multiple-input multiple-output underwater acoustic communications," *IEEE J. Ocean. Eng.*, vol. 41, no. 1, pp. 232–242, 2016.
- [31] B. Muquet, Z. Wang, G. B. Giannakis, M. de Courville, and P. Duhamel, "Cyclic prefixing or zero padding for wireless multicarrier transmissions?" *IEEE Trans. Commun.*, vol. 50, no. 12, pp. 2136–2148, 2002.
- [32] G. H. Golub and C. F. Van Loan, Matrix computations. Johns Hopkins University Press, 2012.